Evolution of soil moisture spatial structure in a mixed vegetation pixel during the Southern Great Plains 1997 (SGP97) Hydrology Experiment

B. P. Mohanty

U.S. Salinity Laboratory, Riverside, California

J. S. Famiglietti

Department of Geological Sciences, University of Texas at Austin, Austin, Texas

T. H. Skaggs

U.S. Salinity Laboratory, Riverside, California

Abstract. Different factors contribute to soil moisture variability at different space scales and timescales, including soil properties, topography, vegetation, land management, and atmospheric forcings, such as precipitation and temperature. Field experiments supported by adaptive geostatistical and exploratory analysis, including categorical elimination of different governing factors, are needed to bring new insight to this important hydrologic problem. During the Southern Great Plains 1997 (SGP97) Hydrology Experiment in Oklahoma, we investigated the within-season (intraseasonal) spatiotemporal variability of surface (0–6 cm depth) soil moisture in a quarter section (800 m × 800 m) possessing relatively uniform topography and soil texture but variable land cover. Daily soil moisture measurements were made between June 22 and July 16 using portable impedance probes in a regular 7 × 7 square grid with 100-m spacings. Initially, the land cover was split between grass and wheat stubble; row tilling on June 27 converted the wheat stubble to bare ground. Geostatistical and median polishing schemes were used to analyze the within-season evolution of the spatial structure of soil moisture. The effects of daily precipitation, variable land cover, land management, vegetation growth, and microheterogeneity including subgrid-scale variability were all visible in the analysis. Isotropic spatial correlation range for soil moisture varied between <100 m (for nugget and subgrid-scale variability) and >428 m (for spherical and Gaussian models) within the 4-week-long SGP97 experiment. The findings will be useful for assessing remotely sensed soil moisture data collected during the SGP97 Hydrology Experiment in mixed vegetation pixels.

1. Introduction

Surface soil moisture plays a pivotal role in the global water and energy balance. Understanding the spatiotemporal variability of surface soil moisture at different scales in space (plot, field, watershed, region, and continent) and time (day, month, season, year, decade, and century) is an increasingly critical issue in the hydrologic sciences. Using different sampling designs (25-m × 25-m grid, and 2- and 5-m spacings in two transects), *Loague* [1992] found little spatial structure in soil moisture for different space scales and timescales in R-5 catchment in the southern Great Plains region. *Charpentier and Groffman* [1992] studied the effects of topography and level of soil moisture on the variability of soil moisture within remote sensing pixels (66 m × 66 m) during the First International Satellite Land Surface Climatology Project (ISLSCP) Field Experiment (FIFE) in Kansas during 1987 and 1989. Geostatistical analysis for several dates/pixels did not show any consistent patterns of spatial dependence with either topography or level of moisture. They suggested that the within-pixel

soil moisture variability was not directly influenced by topography or aspect but more likely due to the variation in soil texture, soil structure, plant distribution, and/or previous disturbance history. *Vinnikov et al.* [1996] presented a spatiotemporal analysis of soil moisture in Russia. Although their long-term (>30 years) data encompassed a large region (30,000 km²), they could not distinguish the effect of spatial inhomogeneity of vegetation, soil type, and topography because of limited sample size, suggesting the variability as part of the natural random error. On the basis of the evolving complexity of the problem, *Georgakakos and Baumer* [1996] recommended the hydrology community for continuation of soil moisture measurement at different space scales and timescales.

Topography played a dominant role in the design and analysis of many contemporary soil moisture variability studies at small catchment or hillslope scales [e.g., *Western et al.*, 1998a, 1998b; *Western et al.*, 1999a, 1999b; *Mohanty et al.*, 2000]. In these studies, a major significance for scaling spatial field of soil moisture is the existence of connectivity and nonstationarity. These characteristics introduce uncertainty about applicability of standard geostatistical tools. More recently, using resampling analysis, *Western and Bloschl* [1999] showed that the apparent variance increases with increasing extent, de-

creases with increasing support, and does not change with spacing, while apparent correlation lengths always increase with spacing, extent, or support. They also concluded that geostatistical techniques are applicable to organized soil moisture fields and that the bias is predicated equally well for organized and random soil moisture patterns. In their geostatistical analysis of seasonal soil moisture patterns in the Tarrawarra catchment in Australia, *Western et al.* [1998a] gave a comparative review of the findings of similar soil moisture variability studies, including *Hills and Reynolds* [1969], *Bell et al.* [1980], *Warrick et al.* [1990], *Loague* [1992], *Rajkai and Ryden* [1992], *Charpentier and Groffman* [1992], and *Nyberg* [1996]. An important point in their discussion was that large variation among these studies with respect to spatial correlation (ranging from zero correlation to a correlation length of 650 m and a sill of 1–$110\%^2$) could possibly be due to one or more of the following reasons: large sample spacing unable to capture the correlation range; too small support and/or sample size to reliably estimate spatial correlation; measurement error greater than the spatial variability; and/or differences in sampling scales, measurement techniques, climate, vegetation, and topography.

Although their relative importance changes from one scale to another, the most important factors determining water transport in soil include precipitation, soil moisture content, soil temperature, overland flow, downward infiltration, upward exfiltration or evapotranspiration, and the soil hydraulic and soil thermal properties. Quantifying the effects of the individual factors on large-scale hydrologic behavior requires a series of detailed experiments at different space scales and time-scales. Once the individual contributions of soil, landscape, vegetation, temperature, precipitation, and other factors are studied, prudent assimilation of different types of data from different sources or platforms should provide a means to predict the large-scale dynamics of soil moisture variability. As part of this larger goal, we conducted several ground-based spatiotemporal variability studies in selected quarter sections during the Southern Great Plains 1997 (SGP97) Hydrology Experiment in central Oklahoma. An overview of the ground-based investigation of soil moisture variability within different remote sensing footprints across the SGP97 focus region (250 km × 60 km) is given elsewhere [*Famiglietti et al.*, 1999]. Also, we presented the analysis of limited high-resolution ground data in a smaller field (400 m × 160 m) where spatial distributions of soil moisture were dominated by landscape positions without any field-scale spatial structure [*Mohanty et al.*, 2000]. The primary focus of this paper is to study the within-season (intraseasonal) evolution of the spatial structure of soil moisture in a mixed vegetation quarter section (800 m × 800 m) possessing uniform soil texture and topography but time-varying land cover, precipitation, and soil temperature. Also, the temporal stability of spatial structure of the surface soil moisture content, with and without the dynamic factors (i.e., land cover, precipitation, and soil temperature), is investigated. A secondary objective of this study is to develop a simple, physically interpretable, resistant (to outlier) scheme for the analysis of spatiotemporal soil moisture data.

2. Southern Great Plains 1997 (SGP97) Hydrology Experiment

The SGP97 Hydrology Experiment was a coordinated collaborative effort by an interdisciplinary science team spon-

sored by the National Aeronautic and Space Administration (NASA), the U.S. Department of Agriculture–Agricultural Research Service (USDA-ARS), the National Oceanic and Atmospheric Administration (NOAA), the Department of Energy (DOE), the National Science Foundation (NSF), and other agencies. A detailed description of the experimental plan, including the different scientific objectives of the mission, can be found elsewhere (see the World Wide Web at http://hydrolab.arsusda.gov/sgp97/). The southern Great Plains region in Oklahoma was selected for this experiment because it is one of the best instrumented sites in the world for surface soil moisture, hydrology, and meteorology. A key objective of the SGP97 soil moisture team was to develop a good understanding of the spatiotemporal variability of soil moisture at a hierarchy of scales. During the SGP97 hydrology experiment (June 18 to July 18, 1997) the soil moisture content was measured over an area >10,000 square km² at different resolutions using different platforms, including an aircraft-based push broom type L band electronically scanned thinned array radiometer (ESTAR) measuring at a resolution of 800 m × 800 m, a truck-mounted microwave remote sensor measuring at a scale of 2.5 m × 2.5 m, and others. A complete list of remote sensors used and their specifications can be found in the SGP97 experimental plan (http://hydrolab.arsusda.gov/sgp97/). Concurrent to remote sensing, point-scale soil moisture measurements were made using (ground-based) gravimetric or electromagnetic techniques. Most of the ground measurement activities were centered around three key facilities, namely, the Agricultural Research Service (ARS) facilities in the Little Washita (LW) watershed southwest of Chickasha, the ARS facility at El Reno (ER), and the Atmospheric Radiation Measurement cloud and radiation test beds (ARM CART) central facility (CF) near Lamont. A total of 9–14 gravimetric soil moisture measurements were made daily at 49 different quarter sections (800 m × 800 m). At selected SGP97 quarter sections a larger number of measurements were made using impedance probes. Recent advances in portable time domain reflectometry (TDR) and impedance probe technologies are making it increasingly possible to monitor the surface soil moisture content at a large number of locations within limited time [e.g., *Grayson and Western*, 1998; *Nyberg*, 1996; *Robinson and Dean*, 1993]. *Famiglietti et al.* [1999] presented the sample statistics of the extensive spatiotemporal soil moisture data for these quarter sections. A major finding of their study is that the range and temporal dynamics of the variability in moisture content between sites are consistent with variations in soil type, vegetation cover, and rainfall gradients. *Mohanty et al.* [2000] adopted an intensive sampling scheme (800 measurements in 24 hours within an area of 400 m × 160 m) and demonstrated several site-specific characteristics of soil moisture variability at a selected SGP97 field (LW07) with uniform soil and vegetation and gently sloping topography. The results indicated that moisture redistribution across the midslope landscape position was the most significant factor controlling the field-scale spatiotemporal variability of surface moisture. However, no field-scale spatial structure was observed for the (40 m × 40 m) block means of soil moisture in that study. Along these lines, we will discuss in this paper the within-season evolution of the spatial correlation structure of soil moisture with respect to the dynamics of land cover, precipitation, and temperature in a mixed vegetation, row tilled quarter section with uniform soil texture and topography (LW21) during the SGP97 experiment using an extensive sampling protocol. The intensive and exten-
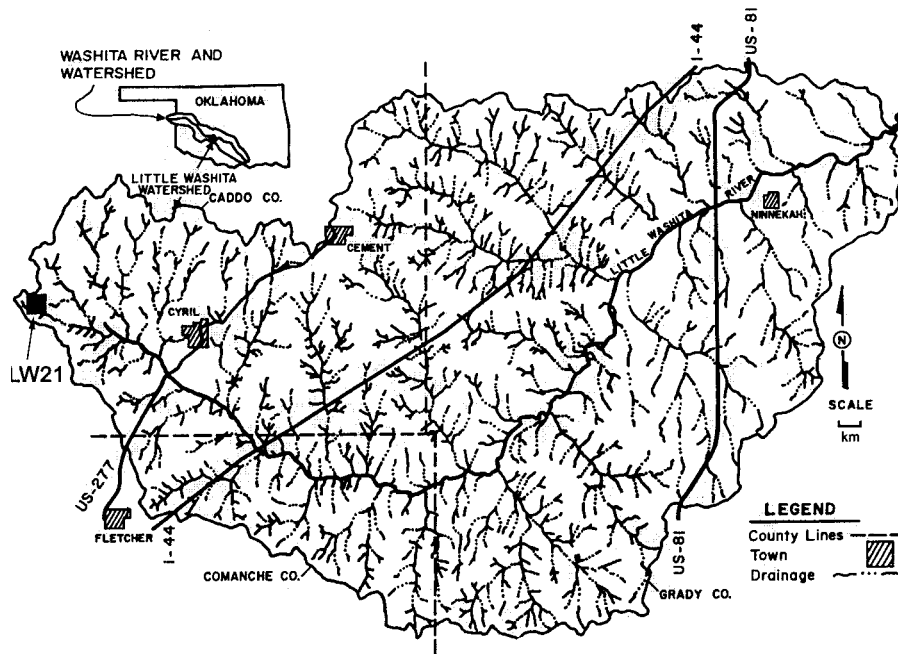
Figure 1. General map of the Little Washita watershed.

sive sampling schemes were designed to provide complementary information on spatiotemporal variability of surface soil moisture at a hierarchy of space scales and timescales under different combinations of soil, topography, vegetation, land management, and climatic conditions. The information is useful for large-scale hydrologic, climatic, and other general circulation studies as well as testing remotely sensed soil moisture data.

3. Experimental Design

The Little Washita watershed (Figure 1) was a critical study area of SGP97. The watershed has been the focus of hydrologic research for over 35 years. The Little Washita watershed covers 610 km^2 and is a tributary of the Washita River in southwest Oklahoma. The watershed is in the southern part of the Great Plains of the United States. The climate is classified as subhumid with an average annual rainfall of 75 cm. The topography of the region is moderately rolling with a maximum relief of ~200 m. Soils include a wide range of textures with large areas of both coarse and fine textures. Rangeland and pasture with significant areas of winter wheat and other crops dominate land use. Additional background information on the watershed are given by *Allen and Naney* [1991] and *Jackson and Schiebe* [1993].

The LW21 field is located near the western edge of the Little Washita watershed (Figure 1). The county soil survey shows the field is predominantly silt loam. Among the quarter sections studied extensively during SGP97, a unique feature of LW21 was its mixed land cover pattern. Initially, two thirds of the field were covered by winter wheat stubble, and the other third, separated by a barbed wire fence, was covered by short native grass (Figure 2). Row tilling on June 27 converted the wheat stubble to bare ground. Thus the LW21 quarter section can be classified as a uniform pixel in terms of soil and a mixed pixel in terms of vegetation/land cover. Here the claim of uniformity in soil properties related to soil moisture dynamics

is only based on soil texture. While we acknowledge the general limitation of this assumption, it is noteworthy that texture relates to hydraulic properties of soil quite significantly [e.g., *Arya and Paris*, 1981; *Cosby et al.*, 1984; *Carsel and Parrish*, 1988; *Schaap et al.*, 1998]. Influence of soil texture on soil hydraulic and retention properties is particularly dominant in the middle to low soil water pressure range. On the other hand, bigger pores (soil structure) dominate the hydraulic properties near saturation. As mentioned below, we skipped sampling during heavy rainfall events, essentially limiting the surface soil moisture dominated by soil texture, which further justifies our assumption of uniform soil. The quarter section is generally flat with <1% slope except for a small upland area in the middle of the grass field with 3–12% slope. We designed a regular 7 × 7 square grid with 100-m spacings, as shown in Figure 2. The grid spacing was determined on the basis of several factors: (1) available human and technical resources, (2) narrow time window of daily sampling, and (3) prior research results in the same general region showing limited spatial structure of soil moisture at smaller lags [*Loague*, 1992; *Charpentier and Groffman*, 1992]. Posterior analyses of the SGP97 data [*Famiglietti et al.*, 1999; *Mohanty et al.*, 2000] attest these region-specific conclusions. Besides these site-specific items, our design adheres to a general conclusion of *Western et al.* [1999a] that suggested land use/cover may generate spatial variability in soil moisture much larger than that usually encountered owing to topography. The location of the grid resulted in 14 sampling points in the grass field and 35 sampling points in the wheat field. Junction points were identified and flagged using a Differential Global Positioning System (DGPS). The DGPS system was operated by using the correction signal transmitted by radio beacon from a reference station in Sallisaw, Oklahoma, which is part of a network maintained by the U.S. Coast Guard. During the SGP97 hydrology campaign (June 18, 1997 to July 18, 1997), the volumetric moisture content in the 0–6-cm surface soil layer was mea-
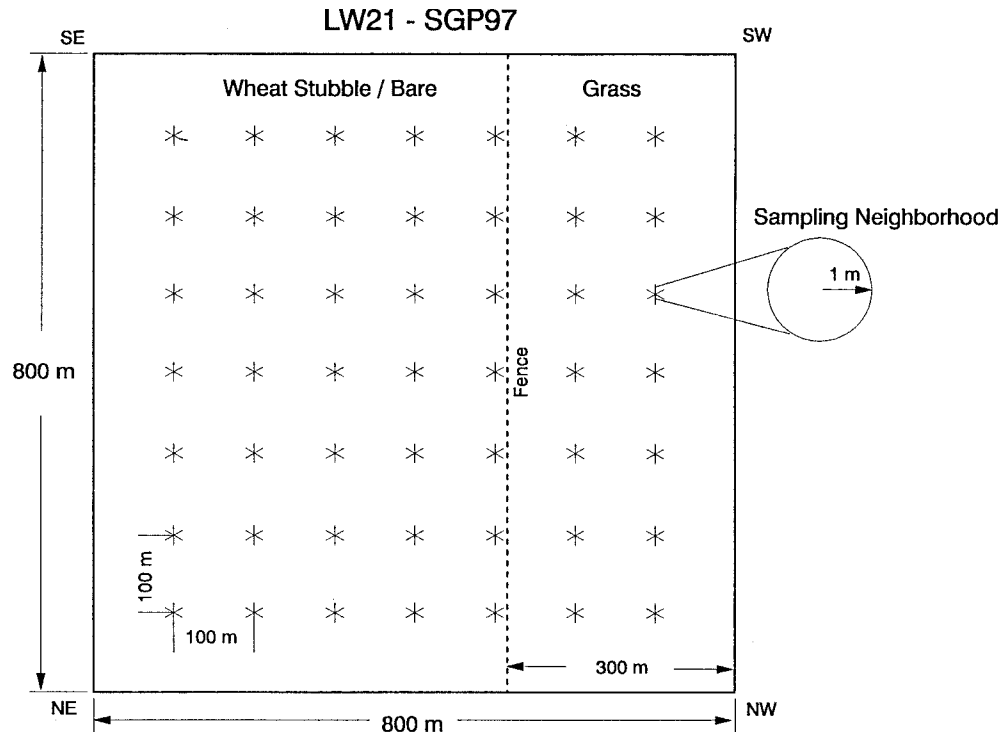
Figure 2. Soil moisture sampling grid in LW21.

sured daily at the 49 (7 × 7) sampling points following a serpentine sequence starting at the NE or NW corner of the field. Sampling was suspended during rain events or when agricultural activity (cultivation on June 27) posed a significant safety concern. In total, 17 sets of daily soil moisture data were collected. Two 2-person teams accomplished the daily sampling in 3–4 hours each afternoon using two sets of portable impedance probe and a DGPS unit.

Soil moisture was measured using a commercially available impedance probe (theta probe soil moisture sensor, type ML1, Delta-T Devices, Cambridge, England). This device measures soil moisture in the 0–6-cm soil layer, which closely matches the depth of other gravimetric and remote sensing measurements (0–5 cm) made during the SGP97 campaign. The probe uses a simplified voltage standing wave method to determine

the relative impedance of its sensing head (which consists of four sharpened, 6-cm-long stainless steel wire rods) and thus the dielectric constant of the soil matrix, which is related to the volumetric water content of soil. Further details of the design and application of this technique are given by *Gaskin and Miller* [1996]. Calibration of this method around the SGP97 region by our collaborators indicated close agreement with the calibration curve of *Gaskin and Miller* [1996]. Thus we used the same curve without any site-specific reevaluation. Two probes were used for our measurements at the LW21 field. In situ evaluation showed no significant difference between the two probes; the analyses in the following sections are based on pooled data from both probes. Statistical properties of this data set are summarized in Table 1.

A weather station (APAC, Oklahoma Mesonet) located

Table 1. Statistics of Raw Volumetric Soil Moisture Content at LW21, SGP97

Date	N	Mean	Variance	Maximum	Minimum	Skewness	Kurtosis
June 22, 1997	49	24.37	17.75	34.16	15.21	.345	−.101
June 24, 1997	49	25.86	17.50	35.23	18.13	.148	−.701
June 26, 1997	49	22.81	30.89	36.87	10.07	.017	.237
June 28, 1997	49	23.80	34.05	38.65	9.56	.020	.325
June 29, 1997	49	21.27	39.93	36.40	8.85	.301	−.325
June 30, 1997	49	18.11	60.84	35.55	3.93	.060	−.631
July 1, 1997	49	15.58	44.06	28.31	2.26	−.047	−.718
July 2, 1997	49	14.83	47.91	32.59	1.27	.454	.453
July 3, 1997	49	11.29	58.95	27.23	0.00	.032	−.928
July 6, 1997	49	10.52	58.95	28.00	0.00	.313	−.634
July 7, 1997	49	9.82	47.33	26.93	0.00	.022	−.739
July 8, 1997	49	9.28	56.70	30.69	0.00	.512	−.219
July 11, 1997	49	27.02	36.97	39.79	8.99	−.369	.091
July 12, 1997	49	23.25	37.70	33.12	1.86	−.891	1.753
July 13, 1997	49	20.41	41.86	33.06	4.69	−.151	−.344
July 14, 1997	49	18.88	48.44	34.10	1.68	−.028	−.339
July 16, 1997	49	19.04	21.16	29.42	11.02	.191	−.767

within 1 km of the northwest corner of the LW21 field is assumed to provide field-representative atmospheric variables including precipitation, evaporation, and radiation. Spatial variability of atmospheric variables is neglected in this study. We used a portable single-probe thermocouple thermometer (Baranant 100, Model 600-2820, Industrial Instruments and Supply, Southampton, Pennsylvania) to measure the spatial distribution of soil temperature across the field. We measured soil temperature on three dates (June 22, July 13, and July 14) at 14 grid nodes within each land cover. At the beginning of the campaign the field was covered in grass and wheat stubble. Subsequently, the wheat field was row tilled on June 27, changing the land cover to bare land.

4. Spatiotemporal Data Analysis and Discussion

The observed spatiotemporal distribution of surface soil moisture likely results from several intrinsic and extrinsic factors, including soil properties, topography, land covers, atmospheric forcings, microheterogeneity, and experimental error. Broadly, these factors can be classified as dynamic or static depending on whether or not they change with time [*Reynolds*, 1970]. Although in a general sense the soil properties of LW21 can be identified as a static factor, row tilling on June 27 changed the porosity of the wheat field topsoil. Similarly, field topography was unchanged at a larger scale, while microtopography was manipulated because of cultivation. On the other hand, land cover was dynamic because of the normal growth and decay of vegetation and because of drastic changes (wheat stubble to bare) caused by cultivation. Thus several of the dynamic components of soil, topography, and vegetation are related to land management and can be grouped as a management factor. Precipitation and other atmospheric factors, including evaporative, radiative, and thermal transfer of moisture, are always dynamic. Additional factors contributing to the spatiotemporal evolution of the (observed) soil moisture field include microheterogeneity, subgrid-scale variability, and experimental error. As soil, topography, and atmosphere were assumed uniform across the LW21 quarter section, interaction terms among these components and land cover were neglected. We expressed the gridded surface soil moisture data $\theta^{z,t}$ as an additive model of these static and dynamic components. Simplifying the more general three-dimensional exploratory data analysis scheme of *Mohanty and Kanwar* [1994], the regionalized variable $\theta^{z,t}$ was written as

$$\theta^{z,t} = \theta^{z,t}_{\text{mean}} + \theta^{z}_{\text{soil}} + \theta^{z}_{\text{topo}} + \theta^{z,t}_{\text{vege}} + \theta^{z,t}_{\text{manag}} + \theta^{z,t}_{\text{atmsph}} + \theta^{z,t}_{\text{err}},$$

$$(1)$$

where

$\theta^{z,t}$ regionalized variable (volumetric soil moisture content) at spatial location z and time t;

$\theta^{z,t}_{\text{mean}}$ mean soil moisture content at spatial location z and time t;

θ^{z}_{soil} contribution of (static) soil factor at spatial location z;

θ^{z}_{topo} contribution of (static) topographic factor at spatial location z;

$\theta^{z,t}_{\text{vege}}$ contribution of (dynamic) vegetation factor at spatial location z and time t;

$\theta^{z,t}_{\text{manag}}$ contribution of (dynamic) management factor at spatial location z and time t;

$\theta^{z,t}_{\text{atmosph}}$ contribution of (dynamic) precipitation and other atmospheric forcings at spatial location z and time t;

$\theta^{z,t}_{\text{err}}$ microheterogeneity including subgrid-scale variability and experimental error at spatial location z and time t, a (dynamic) random component that may or may not inherit the spatiotemporal structure of the state variable.

Mohanty and Kanwar [1994] used x, y, and z spatial coordinates for the exploratory analysis of a three-dimensional spatial data set. In this case, we used one spatial coordinate (z) and one temporal coordinate (t), with the spatial coordinate locating vegetation type and other space-varying factors and the time coordinate identifying time-varying factors, such as land management, precipitation, and vegetation growth. A caveat for this conceptual approach is that the volumetric soil moisture is treated solely as a statistical variable without considering geophysical processes explicitly. The physical processes are implicitly embedded in the various factors that comprise the state variable. For example, the soil factor lumps the effects of soil water retention, hydraulic, and thermal properties; the topography factor lumps the effects of overland flow, subsurface base flow, and aspect-driven radiative transfer of soil moisture; the vegetation factor lumps the effects of land cover and evapotranspiration, and so forth.

To study the temporal evolution of the spatial structure of the soil moisture content and the contribution of different static and dynamic factors at the field site (LW21), we adapted a resistant (to outlier) median polishing approach [*Mohanty and Kanwar*, 1994] to filter out any known space-dependent and time-dependent contribution(s) from the raw data. For example, the vegetation factor was filtered using

$$\theta^{z,t}_{-\text{vege}} = \theta^{z,t} - \langle \theta^{t}_{\text{vege}(i)} \rangle, \tag{2}$$

where $\theta^{z,t}_{-\text{vege}}$ is volumetric soil moisture content at spatial location z and time t with the vegetation factor removed and $\langle \theta^{t}_{\text{vege}(i)} \rangle$ is median volumetric soil moisture content under vegetation type i for time t. For our field campaign the median soil moisture content $\langle \theta^{t}_{\text{vege}(i)} \rangle$ for the wheat stubble (June 22 to June 27), bare (June 28 to July 16), and grass (June 22 to July 16) fields are presented in Figure 3. Figure 3 reveals that the median soil moisture content under wheat stubble was generally higher than that under grass. However, once the wheat field was cultivated (June 27), the opposite trend was established for the rest of the sampling period; the median soil moisture content for the grass field was higher than that for the bare land. A possible reason for this trend is the variation in distribution and density of roots and canopies for different land covers. We used a classical semivariogram estimator [*Matheron*, 1963] to evaluate the two-dimensional spatial correlation structure for the raw (inclusive of vegetation factor) and the median polished (excluding vegetation factor) soil moisture data for each sampling date ($t = 1 \ldots T$). Details on the geostatistical procedure and exploratory analysis can be found elsewhere [*Journel and Huijbregts*, 1978; *Cressie*, 1993; *Mohanty and Kanwar*, 1994]. The two-dimensional isotropic semivariogram estimate $\gamma^{*}(h_i)$ for lag distance class h_i is defined as

$$\gamma^{*}(h_i) = \frac{1}{2N(h_i)} \sum_{i=1}^{N(h_i)} [\theta(z) - \theta(z + h_i)]^2, \tag{3}$$

where $N(h_i)$ is the number of pairs of soil moisture [$\theta(z)$, $\theta(z + h_i)$] measurements separated by a lag range h_i. Plot-
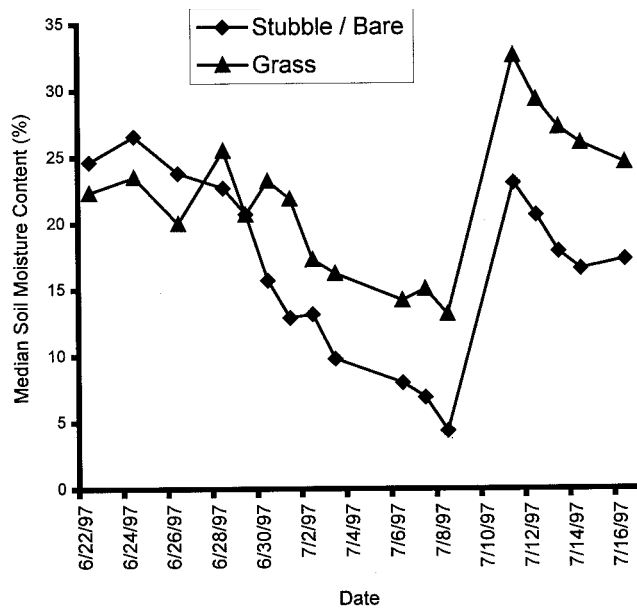
Figure 3. Temporal distribution of median soil moisture contents under different vegetation and land covers.

ting the experimental semivariograms across time revealed the evolution of the spatial structure and other characteristic features of the soil moisture field at LW21 (Figure 4). Generally, with large pixel sizes for remote sensors, researchers lump within-pixel variability of soil moisture because of variation in land cover, soil, topography, and atmospheric factors. Plotting both raw and median polished semivariograms will provide a better insight to identify the contribution of different factors in spatial organization of soil moisture. Our reasoning is based on supporting evidence by other soil moisture/hydrology research. For example, *Western and Bloschl* [1999] developed semivariograms for nonstationary data sets to point out the topographic influence on soil moisture pattern. Most importantly, comparing the resampling analysis and geostatistical analysis results, they concluded that geostatistical techniques are, indeed, applicable to the organized (nonrandom) soil moisture patterns. Also, *Kavvas* [1999] pointed out that nonstationarity may translate to stationarity with the increase in scale also known as the phenomenon of coarse graining of the hydrologic processes. Isotropic semivariograms for raw and median polished soil moisture data were estimated using a geostatistical software, GS$^+$ (Gamma Design Software, Plainwell, Michigan). Lag distances were grouped for producing semivariogram estimations with reasonably large number of data pairs (i.e., 100 m, 84; 170 m, 142; 256 m, 226; 349 m, 218; 428 m, 164, as shown for June 22, 1997, Figure 4). While experimental semivariograms for different dates in Figure 4 are presented using variable *y* axis to demonstrate the contribution of split vegetation factor at different lag distances, Table 2 presents the best fit theoretical models for these isotropic semivariograms. A nonlinear least squares technique was used to fit the theoretical models to experimental semivariograms. Besides microheterogeneity including subgrid-scale (i.e., 0–100 m) variability, an isotropic spherical or Gaussian model was found to describe the daily soil moisture semivariograms reasonably well with evolving correlation lengths ranging from <100 m (for a nugget including subgrid-scale variability) to 2829 m with Gaussian structure. Modeled spatial correlation length (e.g., 2829 m) larger

than the maximum lag distance used in experimental semivariogram estimation (i.e., 428 m) merely indicates the (hypothetical) extrapolated soil moisture field for model fitting. In other words, in these instances, soil moisture is correlated for the entire (observed) lag distance (428 m) used in experimental semivariogram computation. Typically, these isotropic models are defined in terms of nugget variance C_0, sill (nugget variance C_0 plus structural variance C), and correlation range parameter A_0. For a spherical model, A_0 defines the spatial correlation length, whereas for an asymptotic Gaussian model, spatial correlation length is $\approx 3A_0$. For the sake of completeness, we briefly describe these theoretical models here. Detailed characteristics of these models can be found in standard geostatistics texts [e.g., *Journel and Huijbregts*, 1978].
Spherical isotropic

$$\gamma(h) = \begin{cases} C_0 + C[1.5(h/A_0) - 0.5(h/A_0)^3] & h \leq A_0 \\ C_0 + C & h > A_0 \end{cases} \quad (4)$$

Gaussian isotropic

$$\gamma(h) = C_0 + C[1 - \exp(-h^2/A_0^2)]. \quad (5)$$

In the following, we walk through the daily semivariograms (Figure 4) and probe the governing factors responsible for their dynamics. Note that we refer to the model range here for comparison between dates, even if practical range remains the same. Semivariograms for raw and median polished data on June 22 exhibited spatial structure with a correlation length (range) of ~570 m (Table 2). Furthermore, the difference in the raw and median polished semivariograms at smaller lags was insignificant compared to the difference at larger lags. Five millimeters of precipitation fell between June 22 and June 23 (Figure 5), and the June 24 semivariograms again diverge with increasing lag distance but have a smaller correlation range (i.e., 361 m for raw or <100 m for median polished data) than the June 22 semivariograms. On both dates (June 22 and 24), microheterogeneity including subgrid-scale variability plus structural variability ($C_0 + C$) was relatively low compared to that for the succeeding sampling dates. Following a dry spell (no precipitation between June 23 and June 26), the June 26 semivariograms showed a somewhat Gaussian pattern with increased total variability ($C_0 + C$) and higher spatial correlation length for both raw and median polished data. On the following day (June 27), wheat stubbles were removed by row tilling. The semivariogram on June 28 showed a dramatic increase for small lags, indicating that microheterogeneity including subgrid-scale variability C_0 was dominating the spatial structure of surface soil moisture (i.e., $C_0/(C_0 + C) \approx 1$). The possible reasons for enhanced microheterogeneity are analytical errors because of the difficult conditions to measure soil moisture of 0–6-cm depth and/or the inappropriate calibration curve in the freshly tilled soil. However, we have no supporting data to either accept or reject these hypotheses. The semivariance estimates for larger lags remained similar before (June 26) and after (June 28) cultivation. A large (15 mm) rainfall event on June 28 reduced the relative contribution of microheterogeneity ($C_0/(C_0 + C)$) and somewhat reestablished the spatial structure to the precultivation level on June 29. Presumably, the return to the precultivation structure is due to uniform rainfall across the LW21 quarter section that masked the tillage differences. Another important observation for the June 29 semivariograms is the minimal vegetation effect (i.e., no difference between the raw and median polished semivar-
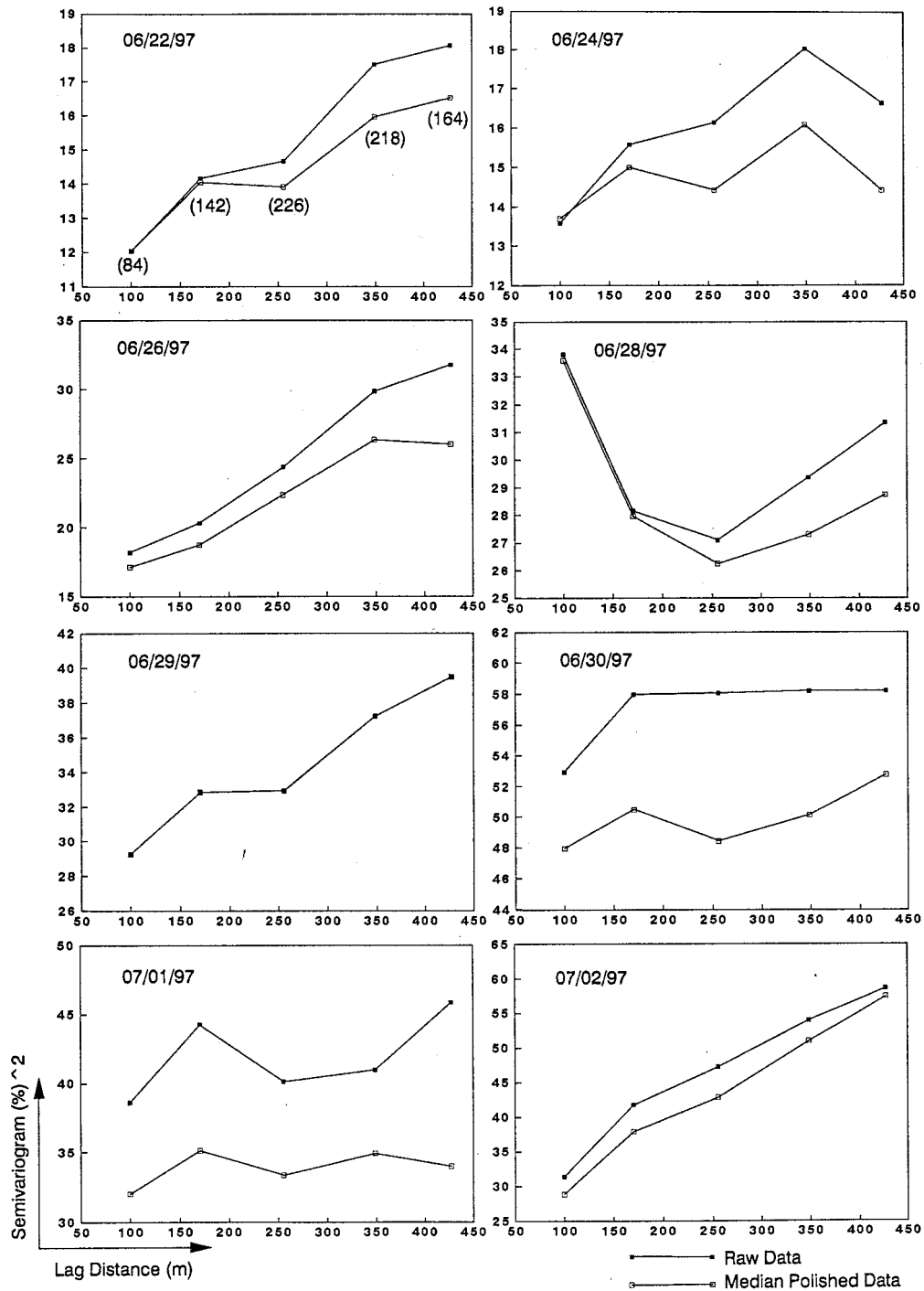
Figure 4. Daily isotropic experimental semivariograms of raw (including vegetation factor) and median polished (excluding vegetation factors) data showing the time evolution of spatial structure of surface soil moisture at LW21. Numbers in the parentheses show the data pairs used for semivariogram estimation for different lag distances. The same number of data pairs were used for each semivariogram estimation.

iograms), which is consistent with the fact that both the land cover types (i.e., bare and grass) had same median soil moisture content (Figure 3). On the next day (June 30) both semivariograms ($C_0 + C$) increased for all lag distances while the correlation lengths decreased (i.e., 153 m for raw data and <100 m for median polished data). However, the differences between the raw and median polished semivariograms were enlarged, indicating a higher contribution of the (split) vege-

tation/land cover factor. The spatial correlation structures became less consistent after July 1. The July 2 semivariograms showed a spherical trend. One day later (July 3), the semivariograms swing back to nuggets (C_0) with a significant contribution from split vegetation. A mild rainfall (3 mm) on July 4 reduced the vegetation (i.e., difference between raw and median polished data) and microheterogeneity ($C_0/(C_0 + C)$) contributions in the semivariograms. During the period be-
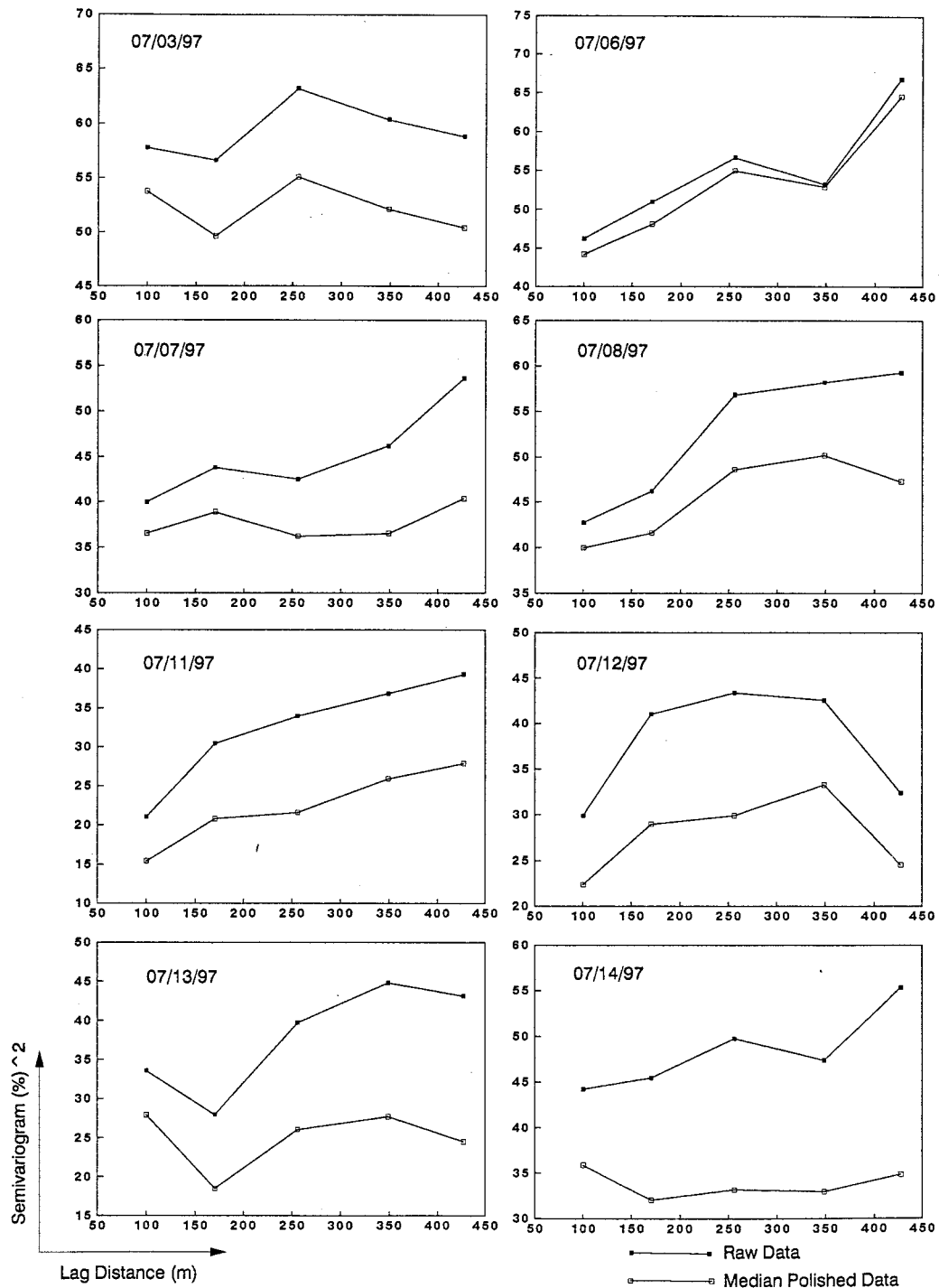
Figure 4. (continued)

tween July 6 and July 11 the soil moisture spatial structure evolved slowly, with a moderate rainfall (9 mm) on July 9 further dampening the effects of microheterogeneity. The last week of our campaign (July 12–16) had several mild rainfall events, and the soil moisture correlation structure evolved toward a spherical model with enlarged vegetation contributions. The heightened vegetation effects may be due to increased growth of grass during this period. On July 14, spatial correlation length for raw data reached a maximum of 2829 m with a best fit Gaussian model. Overall, distinct differences were found between daily spatial structures along the month-long

SGP97 campaign driven by the dynamics of precipitation, land cover, and vegetation. Moreover, microheterogeneity including subgrid-scale variability was found to be significant for intraseasonal soil moisture spatial structure at the LW21 field (Table 2). These further reconfirm other related findings of dominant microheterogeneity [*Famiglietti et al.*, 1999] and time instability (B. P. Mohanty and T. H. Skaggs, Spatio-temporal evolution and time-stable characteristics of soil moisture within remote sensing footprints with varying soil, slope, and vegetation, submitted to *Advances in Water Research*, 2000) features of soil moisture at the LW21 field. Furthermore, these
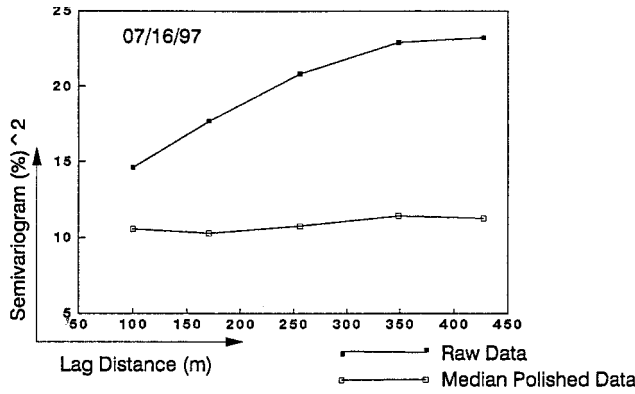
Figure 4. (continued)

findings of within-season (intraseasonal) soil moisture variability and its spatial structure can complement the results of *Western et al.* [1999a] and others who showed seasonal trend in the spatial structure of the soil moisture pattern and attributed to different seasonal processes, including atmosphere-controlled or soil-controlled evapotranspiration or infiltration and topography-controlled lateral flow.

We next compared the results from geostatistical analysis with a few representative contour plots (Figures 6–8) of soil moisture made using linear interpolation of nearest neighbor with surfer package (Golden Software, Golden, Colorado). On June 22 the larger correlation range (as observed in the semi-variogram analysis) corresponds to large patches of wet or dry areas across the quarter section (Figure 6). Also, vegetation and land cover effects are not distinct on this date. The plot for June 28 (Figure 7) showed smaller patches of wet or dry areas because of the high microheterogeneity caused by the cultivation of the wheat field. The plot for July 16 (Figure 8) shows the distinct difference in soil moisture across different land covers (i.e., bare land versus grass cover). Furthermore, the measured surface soil temperature across different land covers showed some amount of difference, which changed for three sampling events (Table 3).

Next, we removed temporal variations due to precipitation and other atmospheric factors using

$$\theta^{z,t}_{-\text{vege-atmosph}} = \theta^{z,t}_{-\text{vege}} - \langle \theta^{z,T}_{\text{atmosph}} \rangle, \qquad (6)$$

where $\theta^{z,t}_{-\text{vege-atmosph}}$ is volumetric soil moisture content at spatial location z and time t with the vegetation and atmo-

Table 2. Parameters and Goodness of Fit of Isotropic Theoretical Models Fitted to Experimental Semivariograms of Volumetric Soil Moisture Content at LW21, SGP97

Date	R/MP[a]	Model Type[b]	Nugget C_0	Sill $C_0 + C$	Nugget/Sill $C_0/(C_0 + C)$	Model Range,[c] m	Practical Range,[d] m	r^2
June 22, 1997	R	S	9.73	18.87	0.515	572	>428	0.957
June 22, 1997	MP	S	10.59	16.98	0.623	569	>428	0.919
June 24, 1997	R	S	11.30	17.26	0.654	361	361	0.873
June 24, 1997	MP	N	15.48		~1	<100	<100	
June 26, 1997	R	G	16.20	35.93	0.451	1752	>428	0.993
June 26, 1997	MP	G	15.02	27.40	0.548	1356	>428	0.973
June 28, 1997	R	N	29.98		~1	<100	<100	
June 28, 1997	MP	N	28.85		~1	<100	<100	
June 29, 1997	R	S	25.90	42.49	0.609	713	>428	0.943
June 29, 1997	MP	S	25.90	42.49	0.609	713	>428	0.943
June 30, 1997	R	S	26.47	43.65	0.606	153	153	0.980
June 30, 1997	MP	N	52.69		~1	<100	<100	
July 1, 1997	R	N	45.19		~1	<100	<100	
July 1, 1997	MP	S	23.90	34.35	0.696	171	171	0.682
July 2, 1997	R	S	20.80	59.15	0.351	494	>428	0.988
July 2, 1997	MP	S	18.30	59.30	0.308	561	>428	0.986
July 3, 1997	R	N	61.04		~1	<100	<100	
July 3, 1997	MP	N	52.20		~1	<100	<100	
July 6, 1997	R	S	40.50	69.38	0.584	740	>428	0.759
July 6, 1997	MP	S	37.80	68.27	0.554	735	>428	0.842
July 7, 1997	R	G	39.10	60.10	0.650	2409	>428	0.829
July 7, 1997	MP	N	39.21		~1	<100	<100	
July 8, 1997	R	G	37.10	59.85	0.619	1077	>428	0.961
July 8, 1997	MP	G	36.08	49.14	0.734	969	>428	0.860
July 11, 1997	R	S	9.90	37.86	0.261	348	348	0.963
July 11, 1997	MP	S	11.22	28.59	0.392	535	>428	0.956
July 12, 1997	R	S	0.10	39.84	0.002	177	177	0.507
July 12, 1997	MP	S	6.59	29.30	0.225	196	196	0.489
July 13, 1997	R	G	28.20	46.65	0.605	1506	>428	0.729
July 13, 1997	MP	N	25.89		~1	<100	<100	
July 14, 1997	R	G	43.70	64.80	0.674	2829	>428	0.753
July 14, 1997	MP	N	33.79		~1	<100	<100	
July 16, 1997	R	S	9.63	23.23	0.414	404	404	1.00
July 16, 1997	MP	N	11.65		~1	<100	<100	

[a]R, raw data; MP, median polished data with split vegetation factor removed.
[b]S, spherical; G, Gaussian; N, nugget.
[c]Range for spherical model is A_0 and for Gaussian model is $\approx 3A_0$.
[d]Practical range indicates the actual correlation length within the 800 m × 800 m field.
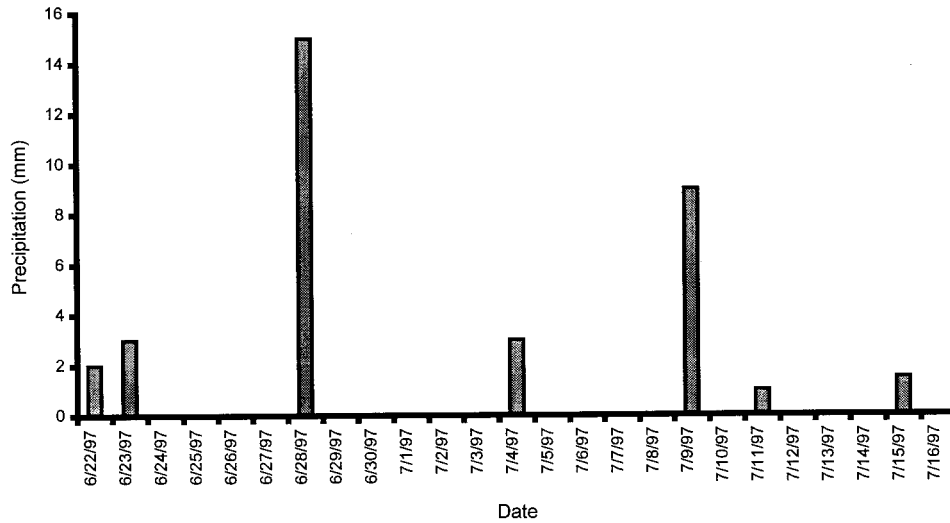
Figure 5. Observed precipitation near LW21 field site (APAC, Oklahoma Mesonet) during the SGP97 campaign.

spheric factors removed and $\langle \theta^{z,T}_{\text{atmosph}} \rangle$ is median volumetric soil moisture content (residual of (2)) for spatial location z over the entire time domain T.

The median polishing (4) also removed the management factor as it was time-dependant. Once the dynamic contributions of vegetation, management, and atmosphere were filtered from the raw soil moisture data, the residual $\theta^{z,t}_{-\text{vege–atmosph}}$ consisted of static factors, such as soil and topography, plus possible contribution from microheterogeneity, subgrid-scale variability, and experimental error. We used an averaging scheme across time adapted from *Mohanty and Kanwar* [1994] for estimating the semivariogram based on $\theta^{z,t}_{-\text{vege–atmosph}}$. An average two-dimensional isotropic semivariogram $\langle \gamma^*(h_i) \rangle$ was calculated as the weighted average of the individual sample semivariograms $\gamma^*_t(h_i)$ for different dates based on the number of pairs $N_t(h_i)$ at each lag class h_i:

$$\langle \gamma^*(h_i) \rangle = \frac{\sum\limits_{t=1}^{T} \gamma^*_i(h_i)\, N_t(h_i)}{\sum\limits_{t=1}^{T} N_t(h_i)} . \tag{7}$$

Note that this time-averaged semivariogram of the median polished residuals is based on the assumption that the soil moisture fields for individual dates are intrinsic random fields. This approach achieves more accurate semivariogram estimates for each lag class because they are based on a greater number of pairs. The average two-dimensional semivariogram was found to be a nugget (Figure 9), indicating the dominance of microheterogeneity including subgrid variability and the relative uniformity of soil and topography at the field site.
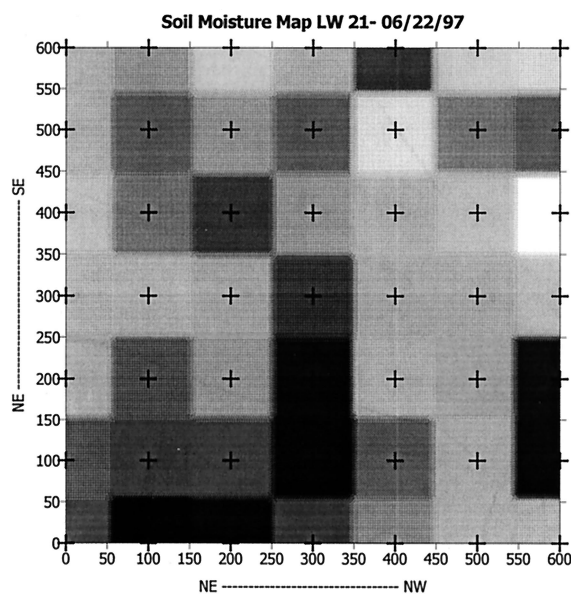
Figure 6. Contour plot of soil moisture content at LW21 on June 22, 1997. Soil moisture contents are in percent, and axes are in meters.
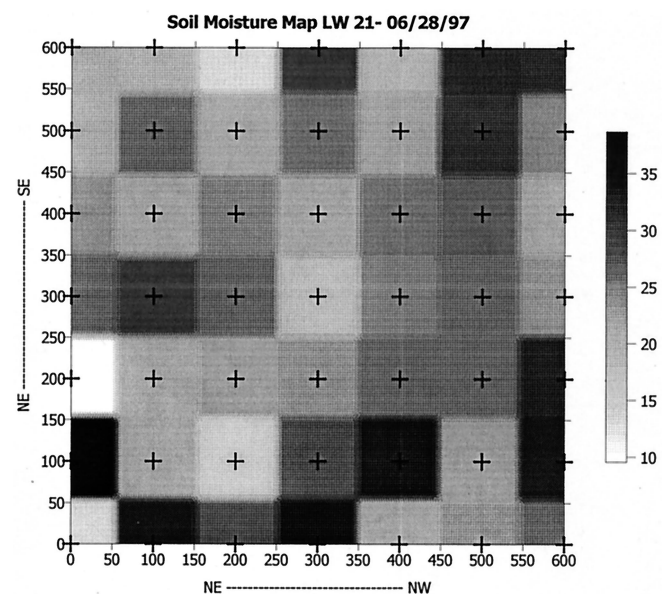
Figure 7. Contour plot of soil moisture content at LW21 on June 28, 1997. Soil moisture contents are in percent, and axes are in meters.

Soil Moisture Map LW 21- 07/16/97
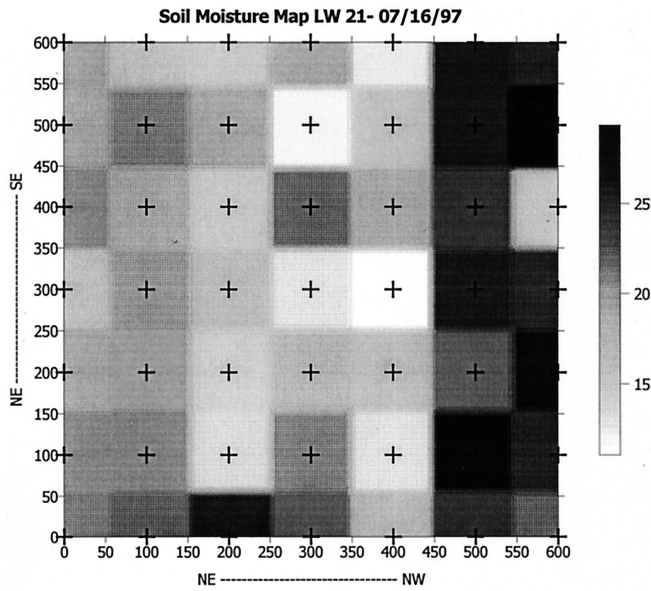
Figure 8. Contour plot of soil moisture content at LW21 on July 16, 1997. Soil moisture contents are in percent, and axes are in meters.

Table 3. Summary Statistics of Soil Temperature at LW21, SGP97

Statistics	June 22, 1997		July 13, 1997		July 14, 1997	
	Stubble	Grass	Bare	Grass	Bare	Grass
Number of observations	14	14	14	14	14	14
Mean	78.43	76.82	87.77	80.94	91.88	83.86
Maximum	81.50	79.80	92.84	89.78	94.28	92.30
Minimum	75.70	74.10	84.20	76.28	89.78	78.26
Variance	2.46	2.65	3.76	11.70	2.10	15.83

5. Summary

As part of the SGP97 hydrology experiment the within-season (intraseasonal) evolution of soil moisture in the LW21 quarter section was investigated using ground-based measurements between June 22 and July 16, 1997. Soil and topography were relatively uniform across the field, while land cover was mixed (wheat stubble and short native grass). During the experiment, row tilling cultivation changed the part of the wheat stubble land cover to bare land. Dynamic atmospheric factors, such as precipitation, radiation, temperature, and wind speed, were assumed or observed to be uniform across the field. The spatiotemporal evolution of the soil moisture field was deter-

mined using daily experimental semivariograms. Clear signatures of temporal changes in vegetation, land management, and precipitation events were found in these semivariograms. Furthermore, contributions from vegetation, land management, and atmospheric governing factors were filtered using a simple and resistant (to outlier) median polishing scheme, resulting in time-averaged semivariograms based on static properties of soil and topography at the field site. Results indicated that dynamics of land cover, vegetation, precipitation, and microheterogeneity dominated the within-season spatial structure and that soil and topography were uniform for the field under investigation. Microheterogeneity including subgrid-scale variability was found to be a significant component of daily soil moisture spatial structure. Intraseasonal spatial correlation length based on daily soil moisture observations fluctuated widely between <100 m (for pure nugget and subgrid-scale variability) and >428 m (2829 m for a Gaussian model). This information will be useful for validation of remotely sensed soil moisture data collected in the mixed vegetation pixels during the SGP97 hydrology experiment. For example, as the nature of spatial organization changes throughout the season, both rules and parameters of operational models need time-dependent adjustments for computing pixel-scale soil moisture content using remote sensors. Also,
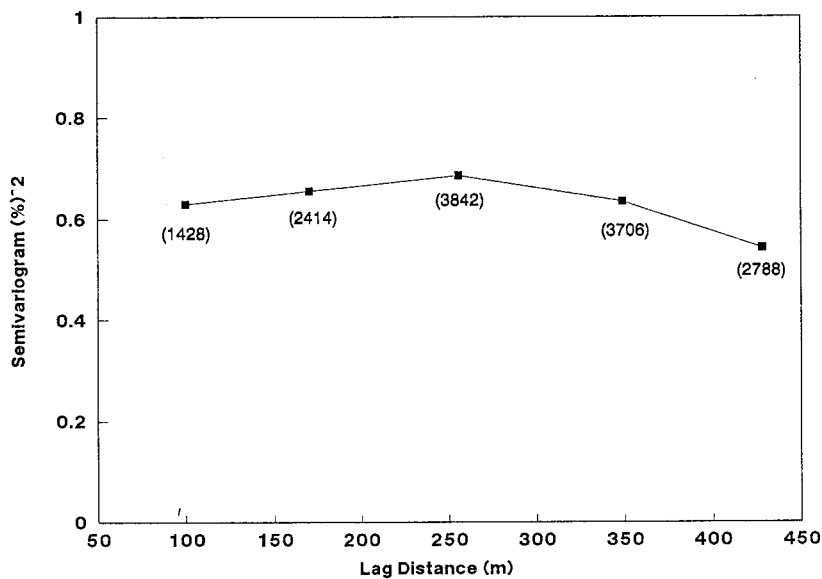
Figure 9. Time-averaged isotropic experimental semivariogram after vegetation and other temporal components were removed from raw soil moisture data using the median polishing scheme. Numbers in the parentheses show the data pairs used for semivariogram estimation for different lag distances.

neglecting the fluctuating behavior of within-season spatial structure of soil moisture and the controlling processes at the pixel-scale may introduce and propagate errors in hydroclimatic modeling at the same or higher spatial (pixel, catchment, watershed, and region) and temporal (season, year, decade, and century) scales. Research efforts should be initiated to address these issues more cohesively.

References

Allen, P. B., and J. W. Naney, Hydrology of the Little Washita River watershed, Oklahoma: Data and analyses, *ARS-90*, 74 pp., U.S. Dep. of Agric., Agric. Res. Serv., Washington, D. C., 1991.

Arya, L. M., and J. F. Paris, A physical model to predict the soil moisture characteristic from particle size distribution and bulk density, *Soil Sci. Soc. Am. J.*, *45*, 1023–1030, 1981.

Bell, K. R., B. J. Blanchard, T. J. Schmugge, and M. W. Witczak, Analysis of surface moisture variations within large field sites, *Water Resour. Res.*, *16*, 796–810, 1980.

Carsel, R. F., and R. S. Parrish, Developing joint probability distributions of soil water retention characteristics, *Water Resour. Res.*, *24*, 755–769, 1988.

Charpentier, M. A., and P. M. Groffman, Soil moisture variability within remote sensing pixels, *J. Geophys. Res.*, *97*(D17), 18,987–18,995, 1992.

Cosby, B. J., G. M. Hornberger, R. B. Clapp, and T. R. Ginn, A statistical exploration of the relationships of soil moisture characteristics to the physical properties of soils, *Water Resour. Res.*, *20*, 682–690, 1984.

Cressie, N. A. C., *Statistics for Spatial Data*, 900 pp., John Wiley, New York, 1993.

Famiglietti, J. S., J. A. Devereaux, C. A. Laymon, T. Tsegaye, P. R. Houser, T. J. Jackson, S. T. Graham, M. Rodell, and P. van Oevelen, Ground-based investigation of soil moisture variability within remote sensing footprints during the Southern Great Plains (1997) Hydrology Experiment, *Water Resour. Res.*, *35*, 1839–1851, 1999.

Gaskin, G. J., and J. D. Miller, Measurement of soil water content using a simplified impedance measuring technique, *J. Agric. Eng. Res.*, *63*, 153–160, 1996.

Georgakakos, K. P., and O. W. Baumer, Measurement and utilization of on-site soil moisture data, *J. Hydrol.*, *184*, 131–152, 1996.

Grayson, R. B., and A. W. Western, Towards areal estimation of soil water content from point measurements: Time and space stability of mean response, *J. Hydrol.*, *207*, 68–82, 1998.

Hills, T. C., and S. G. Reynolds, Illustrations of soil moisture variability in selected areas and plots of different sizes, *J. Hydrol.*, *8*, 27–47, 1969.

Jackson, T. J., and F. R. Schiebe (Ed.), Washita '92 data report, *NAWQL Rep. 101*, U.S. Dep. of Agric., Natl. Agric. Water Quality Lab., Durant, Okla., 1993.

Journel, A. G., and C. J. Huijbregts, *Mining Geostatistics*, 600 pp., Academic, San Diego, Calif., 1978.

Kavvas, M. L., On the coarse-graining of hydrologic processes with increasing scales, *J. Hydrol.*, *217*, 191–202, 1999.

Loague, K., Soil water content at R-5, part 1, Spatial and temporal variability, *J. Hydrol.*, *139*, 233–251, 1992.

Matheron, G., Principles of geostatistics, *Econ. Geol.*, *58*, 1246–1266, 1963.

Mohanty, B. P., and R. S. Kanwar, Spatial variability of residual nitrate-nitrogen under two tillage systems in central Iowa: A composite three-dimensional resistant and exploratory approach, *Water Resour. Res.*, *30*, 237–251, 1994.

Mohanty, B. P., T. H. Skaggs, and J. S. Famiglietti, Analysis and mapping of field-scale soil moisture variability using high-resolution ground based data during the Southern Great Plains 1997 (SGP97) Hydrology Experiment, *Water Resour. Res.*, *36*, 1023–1031, 2000.

Nyberg, L., Spatial variability of water content in the covered catchment at Gardsjon, Sweden, *Hydrol. Proc.*, *10*, 89–103, 1996.

Rajkai, K., and B. E. Ryden, Measuring areal soil moisture distribution with the TDR method, *Geoderma*, *52*, 73–85, 1992.

Reynolds, S. G., The gravimetric method of soil moisture determination, part III, An examination of factors influencing soil moisture variability, *J. Hydrol.*, *11*, 288–300, 1970.

Robinson, M., and T. J. Dean, Measurement of near surface soil water content using a capacitance probe, *Hydrol. Proc.*, *7*, 77–86, 1993.

Schaap, M. G., F. J. Leij, and M. T. van Genuchten, Neural network analysis for hierarchical prediction of soil hydraulic properties, *Soil Sci. Soc. Am. J.*, *62*, 847–855, 1998.

Vinnikov, K. Y., A. Robock, N. Speranskaya, and C. A. Schlosser, Scales of temporal and spatial variability of midlatitude soil moisture, *J. Geophys. Res.*, *101*(D3), 7163–7174, 1996.

Warrick, A. W., R. Zhang, M. M. Moody, and D. E. Myers, Kriging versus alternative interpolators errors and sensitivity to model inputs, in *Field Scale Water and Solute Flux in Soils*, edited by K. Roth et al., pp. 157–164, Birkhäuser Boston, Cambridge, Mass., 1990.

Western, A. W., and G. Bloschl, On the spatial scaling of soil moisture, *J. Hydrol.*, *217*, 203–224, 1999.

Western, A. W., G. Bloschl, and R. B. Grayson, Geostatistical characterization of soil moisture patterns in the Tarrawarra catchment, *J. Hydrol.*, *205*, 20–37, 1998a.

Western, A. W., G. Bloschl, and R. B. Grayson, How well do indicator variograms capture the spatial connectivity of soil moisture?, *Hydrol. Processes.*, *12*, 1851–1868, 1998b.

Western, A. W., R. B. Grayson, G. Bloschl, G. R. Willgoose, and T. A. McMahon, Observed spatial organization of soil moisture and its relation to terrain indices, *Water Resour. Res.*, *35*, 797–810, 1999a.

Western, A. W., R. B. Grayson, and T. R. Green, The Tarrawarra project: High resolution spatial measurement, modeling and analysis of soil moisture and hydrologic response, *Hydrol. Processes*, *13*, 633–652, 1999b.

───────────────

J. S. Famiglietti, Department of Geological Sciences, University of Texas, Austin, TX 78712.

B. P. Mohanty and T. H. Skaggs, U.S. Salinity Laboratory, 450 West Big Springs Road, Riverside, CA 92507. (bmohanty@ussl.ars.usda.gov)